JOURNAL OF RARE EARTHS
Vol. 25, Suppl., Jun. 2007, p. 345

Numerical Study on Flow Field and Temperature Distribution in Growth Process of 200 mm Czochralski Silicon Crystals

Chen Qisheng (陈启生)[1*], Deng Guyu (邓谷雨)[1], Ali Ebadian[2], Vish Prasad[2]
(*1. Institute of Mechanics, Chinese Academy of Sciences, Beijing 100080, China; 2. Department of Mechanical and Materials Engineering, Florida International University, 10555 W Flagler St., Miami, FL 33174, USA*)

Abstract: The melt flow and temperature distribution in a 200 mm silicon Czochralski furnace with a cusp magnetic field was modeled and simulated by using a finite-volume based FLUTRAPP (Fluid Flow and Transport Phenomena Program) code. The melt flow in the crucible was focused, which is a result of the competition of buoyancy, the centrifugal forces caused by the rotations of the crucible and crystal, the thermocapillary force on the free surfaces and the Lorentz force induced by the cusp magnetic field. The zonal method for radiative heat transfer was used in the growth chamber, which was confined by the crystal surface, melt surface, crucible, heat shield, and pull chamber. It was found that the cusp magnetic field could strength the dominant counter-rotating swirling flow cell in the crucible and reduce the flow oscillation and the pulling-rate fluctuation. The fluctuation of dopant and oxygen concentration in the growing crystal could thus be smoothed.

Key words: Czochralski growth; flow field; temperature distributions; cusp magnetic field
CLC number: O782$^+$.5 **Document code**: A **Article ID**: 1002 - 0721(2007) - 0345 - 04

Czochralski (Cz) crystal growth process is the most dominant technique in manufacturing of silicon crystals. Many investigators have devoted their efforts to the improvement of large diameter crystal growth technology[1]. Recently, the Czochralski method is being used to grow silicon single crystal with a diameter of 300 mm and more. Compared to a smaller size, the increase of the crystal diameter from 200 to 300 mm and therefore of the crucible causes the melt flow to be more three-dimensional, time-dependent and turbulent, which in most cases has a detrimental effect on the heat and mass transfer and thereby on the crystal quality[1]. Physics-based modeling and numerical simulation of Cz silicon single crystal growth have been used to understand the characteristics of different factors, and to identify the essential roles they played in improving the crystal quality.

In the early 1980s, the cusp magnetic scheme was introduced to achieve a lower oxygen concentration and good radial uniformity[2, 3] by adopting the advantages of axial magnetic field[4] and transverse magnetic field[5]. Hicks et al.[6] investigated the oxygen transport in magnetic Cz growth of silicon with a non-uniform magnetic field. Sabhapathy and Salcudean[7] studied the melt motions in the silicon Cz growth in an axisymmetric magnetic field. The magnetic field has since been applied to control the stability of the melt convection, the dopant and oxygen concentrations. Ma et al.[8] studied the defects in the crystals grown under three different cusp magnetic fields by using the infrared light scattering tomography. They found that defect density decreases by changing the centre position of the cusp magnetic fields from "outside" to "inside", and they considered the "inside" configuration to be the most effective to obtain a low defects density and oxygen content uniformity. Kim and Lee[9] studied the non-linear behavior of melt motions in different crucible rotation rates and magnetic field strengths. Sim et al.[10] studied the oxygen concentration distribution in the Cz silicon crystals grown in the cusp magnetic field. While the size of the melt enlarges, the oxygen concentration in the crystal increases due to the stronger nature convection caused by the enlarged melt volume, which leads to the increase of the dissolution of oxygen from the crucible into the melt. Moreover, Kishida et al.[11] studied the geostrophic turbulence in the melt under a cusp magnetic field by CCD melt surface observations in a conventional Cz furnace. The Coriolis effect also plays a role in the melt motions, competing with the forced convections by the rotations of crystal and crucible, the buoyancy flow, the Lorentz force-induced convection, and the thermocap-

Received date: 2006 - 11 - 20; **revised date**: 2007 - 04 - 20
Foundation item: Project supported by the National Natural Science Foundation of China (10472126)
Biography: Chen Qisheng (1968 -), Male, Ph.D., Professor; Research field: Fluid mechanics
* **Corresponding author** (E-mail: qschen@imech.ac.cn)

illary convection induced by non-uniform temperature distributions on the free surface.

A multiphase system for a 200 mm industrial silicon growth system consisting of the melt, crystal and furnace was considered. The transport phenomena in the process was focused by using the finite volume method[12, 13]. The zonal method for radiative heat transfer in the growth chamber was used, which was confined by the crystal surface, melt surface, crucible, heat shield, and pull chamber[14]. The effects of a cusp magnetic field on the growth process were studied.

1 Physical and Mathematical Models

A sketch of cusp magnetic field configuration for the growth of silicon single crystals is shown in Fig.1. The cusp magnetic field configuration consists of two circular, current-carrying loops that are located outside the crucible with one placed above the melt surface and another one below the melt surface. The magnetic field is assumed to be axisymmetric and steady, and has no normal component at the free surface. The ambient gases are electrical insulators, while the melt is an electrical conductor[7].

Hicks et al.[6] gave a classical solution for a single current loop and applied it to a two-loop configuration. The magnetic induction is assumed as $B = -B_0 \nabla \varphi$ where potential φ has the form of,

$$\varphi = \sum_{n=0}^{\infty} \alpha_{2n+1} \left(\frac{R'}{R_{\text{coil}}}\right)^{2n+1} P_{2n+1}(\cos\theta) \qquad (1)$$

In (1), $R' = \sqrt{r^2 + (z - z_0)^2}/R_c$, the angel between the vertical axis and the line from the center of loop to the point (r, z), $\theta = \tan^{-1}(r/(z - z_0))$, z_0 is the vertical position of the current loop, $R_{\text{coil}} = R_{\text{coil}}/R_c$, R_{coil} is the radius of the loop, and R_c is the radius of the crucible . The typical magnetic induction , $B_0 = \mu_m I/R_c$, I is the electrical current in the loop, and μ_m is the permeability. $P_n(x)$ is an n degree Legendre polynomial, and

$\alpha_1 = -1/2, \cdots,$

$$\alpha_{2n+1} = \frac{1}{2}(-1)^{(n+1)} \frac{1 \times 3 \times \cdots \times (2n-1)}{2 \times 4 \times \cdots \times 2n}$$

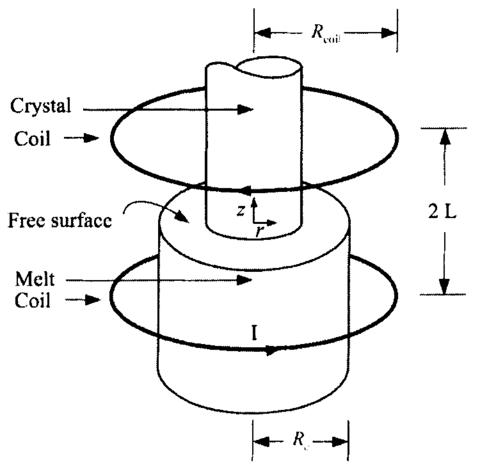

Fig.1 Scheme of a cusp magnetic field configuration

Considering the cusp magnetic field configuration, we can get the magnetic induction,

$$B = -B_0 \nabla (\varphi_1 + \varphi_2) \qquad (2)$$

where subscripts 1 and 2 represent the two coils, respectively.

The components of the current density vector are defined as,

$$J_r = \frac{\sigma_c}{r} \frac{\partial \Psi}{\partial z} \qquad (3)$$

$$J_z = \frac{\sigma_c}{r} \frac{\partial \Psi}{\partial r} \qquad (4)$$

where σ_c is the electric conductivity of the melt, and Ψ is the electric current stream function. The equation for Ψ is then written as,

$$\frac{\partial}{\partial z}\left(\frac{1}{r} \frac{\partial \Psi}{\partial z}\right) + \frac{\partial}{\partial r}\left(\frac{1}{r} \frac{\partial \Psi}{\partial r}\right) = \frac{\partial(\nu B_z)}{\partial z} + \frac{\partial(\nu B_r)}{\partial r} \qquad (5)$$

where ν is the velocity in azimuthal direction. B_r and B_z are the radial and axial components of the magnetic induction, respectively. The remaining component of the current density vector follows from the Ohm Law,

$$J_\theta = \sigma_c(wB_r - uB_z) \qquad (6)$$

After the electric density and the magnetic induction are calculated, the components of Lorentz force can be written as $F = J \times B$:

$$F_r = J_\theta B_z \qquad (7)$$

$$F_\theta = -J_r B_z + J_z B_r \qquad (8)$$

$$F_z = -J_\theta B_r \qquad (9)$$

Assuming that the Boussinesq's approximation can be applied to the buoyancy effect and the flow is incompressible, the governing equations can be written as,

$$\nabla \cdot \mathbf{u} = 0 \qquad (10)$$

$$\frac{\partial}{\partial t}(\rho \mathbf{u}) + (\rho \mathbf{u} \cdot \nabla)\mathbf{u} = -\nabla p + \mu \nabla^2 \mathbf{u} + \rho \mathbf{g} + \mathbf{F} \qquad (11)$$

$$\frac{\partial}{\partial t}(\rho c_p T) + (\rho c_p \mathbf{u} \cdot \nabla) T = k \nabla^2 T + q_{\text{radi}} \qquad (12)$$

where μ is the viscosity, and q_{radi} is the radiative heat transfer source term.

2 Results and Discussion

By employing the classical solution of magnetic field for a single current loop (Eq.1), we are able to calculate the magnetic field for a cusp magnetic-field configuration (Eq.2). Fig.2 shows the magnetic field of a cusp configuration when $B_0 = 1$ T, $L = 1.45R_c$,

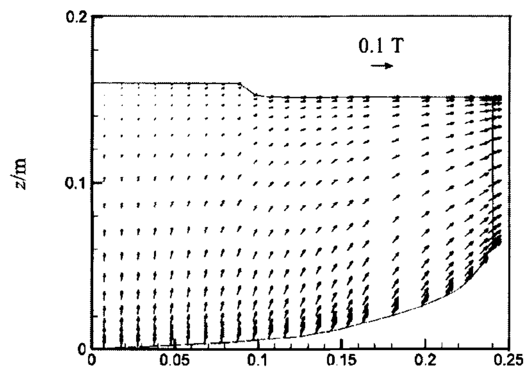

Fig.2 Calculated cusp magnetic field
(when $B_0 = 1$ T, $L = 1.45R_c$, $R_{coil} = 2.9R_c$)

and $R_{coil} = 2.9R_c$. We assume that the magnetic field is unaffected by the fluid motions. After obtaining the magnetic field, the electric current stream function Ψ can be obtained by solving Eq.(5) and the Lorentz force can be obtained from Eqs.(7 ~ 9).

In the following calculation, the crucible radius is $R_c = 0.24$ m, the crystal is rotating at 15 $r \cdot min^{-1}$, and the crucible is rotating in the opposite direction at 2 $r \cdot min^{-1}$. Hartmann number is defined as, $Ha = B_0 R_c \sqrt{\sigma_c / \mu}$. The dimensionless parameters are, $Pr = 0.018$, $Gr = 1.15 \times 10^9$, $Ma = 1.12 \times 10^4$, and $Ha = 20$ corresponding to $B_0 = 0.002$ T. The applied magnetic field for the 200 mm industrial growth is up to 0.04 ~ 0.12 T. Our purpose here is to give some preliminary results on the effects of cusp magnetic field.

The crystal rotation ensures the radial symmetry of thermal condition, so that the crystal grows as a cylinder. Furthermore, the crystal rotation leads to a lower density of any disturbing crystallographically related effects. The crucible rotation is to even out variation in the thermal gradients, dopant distributions, etc., in the azimuthal direction. The crucible rotation also serves the purpose of tuning oxygen concentration, as the crucible wall is the major source of oxygen in the silicon melt.

Figs.3(a) and (b) indicate the melt motions and temperature distribution in a 200 mm Cz silicon single crystal furnace. The high temperatures on the crucible wall result in buoyancy-driven flows in the melt as the Grashof number in this case is very high. Due to the crystal rotation, the fluid under the triple point is pumped radially outwards, competing with the inward flow caused by the melt surface tension. A boundary layer is formed adjacent to the melt/crystal interface known as Ekmon boundary layer. This layer to some extent shields the interface from the vagaries of melt flow thus helping in maintaining uniformity of the interface which is important from the crystal quality point of view.

It is found that the application of a cusp magnetic field can strength the dominant counter-rotating swirling flow cell. Consequently, the oscillation of melt flow and the fluctuation of pumling rate can be reduced. As a result, the fluctuation of dopant and oxygen concentration in the growing crystal can be smoothed.

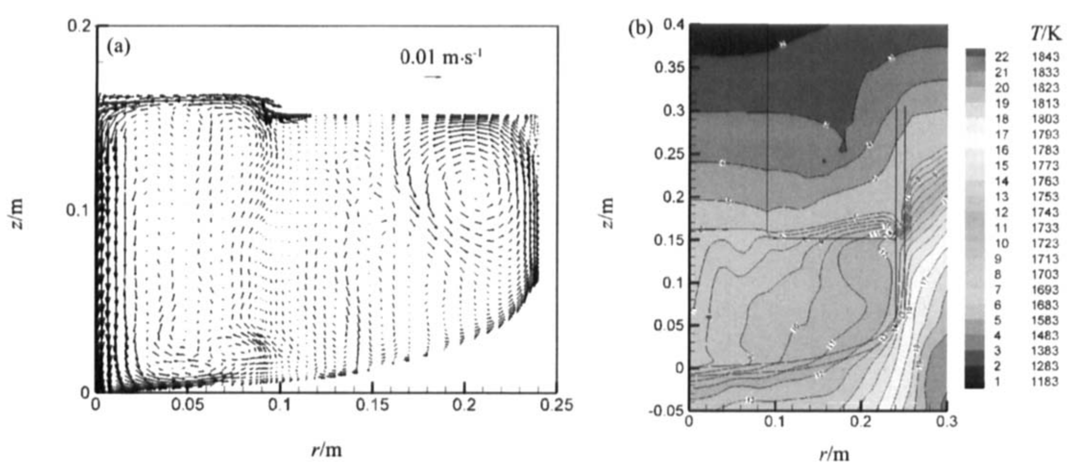

Fig.3 Melt flow (a) and temperature distribution (b) in a 200 mm silicon growth furnace

3 Conclusion

The flow patterns and temperature distributions in a 200 mm Cz silicon growth furnace were modeled and simulated by using the FLUTRAPP (Fluid Flow and Transport Phenomena Program) code, which was based on the non-orthogonal finite-volume scheme. The effects of the cusp magnetic field were studied. It was found that the cusp magnetic field could strength the dominant counter-rotating swirling flow cell, and could reduce the flow oscillation and the pulling rate fluctuation. The fluctuation of dopant and oxygen concentration in the growing crystal could thus be smoothed.

References:

[1] Von Ammon W, Dornberger E, Hansson P O. Bulk properties of very large diameter silicon single crystals [J]. *J. Crystal Growth*, 1999, **198/199**: 390.

[2] Series R W. Effect of a shaped magnetic field on Czochralski silicon growth [J]. *J. Crystal Growth*, 1989, **97**: 92.

[3] Hirata H, Hoshikawa K. Silicon crystal growth in a cusp magnetic field [J]. *J. Crystal Growth*, 1989, **96**: 747.

[4] Hoshikawa K, Kohda H, Hirata H. Homogeneous dopant distribution of silicon crystal growth by vertical magnetic field-applied Czochralski method [J]. *Jpn. J. Appl. Phys.*, 1984, **23**: 37.

[5] Hoshi K, Isawa N, Suzuku T, Ohkubo Y. Czochralski silicon crystals grown in a transverse magnetic field [J]. *J. Electorchem. Soc.*, 1985, **132**: 693.

[6] Hicks T W, Organ A E, Riley N. Oxygen transport in magnetic Czochralski growth of silicon with a non-uniform magnetic field [J]. *J. Crystal Growth*, 1989, **94**: 213.

[7] Sabhapathy P, Salcudean M E. Numerical study of Czochralski growth of silicon in an axisymmetic magnetic field [J]. *J. Crystal Growth*, 1991, **113**: 164.

[8] Ma M, Ogawa T, Watanabe M, Eguchi M. Study on defects in CZ-Si crystals grown under three different cusp magnetic fields by infrared light scattering tomography [J]. *J. Crystal Growth*, 1999, **205**: 50.

[9] Kim J S, Lee T Y. Numerical study of the melt-thermal effect on a silicon crystal in Czochralski growth system [J]. *J. Crystal Growth*, 2000, **209**: 55.

[10] Sim B C, Lee I K, Kim K H, Lee H W. Oxygen concentration in the Czochralski-grown crystals with cusp-magnetic field [J]. *J. Crystal Growth*, 2005, **275**: 455.

[11] Kishida Y, Tamaki T, Okazawa K, Ohashi W. Geostrophic turbulence in CZ silicon melt under CUSP magnetic field [J]. *J. Crystal Growth*, 2005, **273**: 329.

[12] Zhang H, Prasad V. A multizone adaptive process model for low and high pressure crystal growth [J]. *J. Crystal Growth*, 1995, **155**: 47.

[13] Zhang H, Zheng L L, Prasad V, Larson D J Jr. Diameter-controlled Czochralski growth of silicon crystals [J]. *J. Heat Transfer*, 1998, **120**: 874.

[14] Nunes E M, Naraghi M H N. Numerical model for radiative heat transfer analysis in arbitrarily shaped axisymmetric enclosures with gaseous media [J]. *Num. Heat Transfer*, Part A, 1998, **33**: 495.